Enhancement of Tensile Properties of Isotactic Polypropylene Spunbonded Fabrics by a Surface-Modified Silica/Silicone Copolymer Additive

V. CALDAS,[1,*] G. R. BROWN,[1] R. S. NOHR,[2] J. G. MACDONALD,[2] L. E. RABOIN[3]

[1] Department of Chemistry, McGill University, 801 Sherbrooke St. W., Montreal, Québec H3A 2K6, Canada

[2] Kimberly–Clark Corp., 1400 Holcomb Bridge Road, Roswell, Georgia 30076

[3] University of Massachusetts, Polymer Science and Engineering, Amherst, Massachusetts 01003

Received 9 September 1996; accepted 29 January 1997

ABSTRACT: Previous work at Kimberly–Clark Corp. (R. S. Nohr and J. G. MacDonald, Kimberly–Clark Corp., unpublished results, 1990) demonstrated that the addition of an ultrafine-particle (submicron-size), surface-modified silica predispersed in an alkyl silicone to isotactic polypropylene (iPP) results in dramatic improvements in the tensile properties of fibers and spunbonded fabrics. For both fibers and spunbonded fabrics prepared with a high concentration of the low melt flow index (MFI) resin the incorporation of the additive resulted in markedly improved tensile properties. In this article it is shown that under quiescent conditions the surface-modified silica/silicone copolymer additive acts as an effective nucleating agent for iPP. This results in a reduction in the size of the crystalline entities, hence a more homogeneously distributed crystalline phase and load-bearing "tie" molecules. Indeed, scanning transmittance electron microscopy (STEM) studies show that the crystalline entities are substantially smaller at the surface and mid-radius of fibers prepared with additive containing iPP. Furthermore, the bond points of the resulting spunbonded fabrics have a dramatically increased nucleation density and smaller crystallite dimensions. © 1997 John Wiley & Sons, Inc. J Appl Polym Sci **65:** 1759–1772, 1997

Key words: isotactic polypropylene; spunbonded fabrics; silica; silicone; nucleation; additives; tensile properties

INTRODUCTION

A major fraction of the annual production of isotactic polypropylene (iPP) is consumed in the manufacture of fibers and spunbonded fabrics. It is no surprise then, that much effort has been expended in seeking to develop improved formulations and techniques that will result in improved products, both because of market advantage and savings that would result from decreased resin consumption. Inevitably the tensile performance of a spunbonded fabric depends not only on the physical properties of the individual fibers but on the quality of the bond points as well. In addition, consideration must be given to the bond point interface.[1–4]

To improve the tensile properties of a fiber, its physical structure must be affected in a manner that promotes beneficial changes in fiber morphology.[5,6] Furthermore, it is known that certain fiber features can be influenced by acting specifically

Correspondence to: G. R. Brown, University of Northern British Columbia, Chemistry Programme, 3333 University Way, Prince George, British Columbia V2N 4Z9, Canada.

* *Current address:* Domco Ltd., 1001 Yamaska E., Farnham, Québec J2N 1J7, Canada.

 CCC 0021-8995/97/091759-14

on the crystalline phase and its development during the fiber spinning process. For example, the incorporation of additives, *e.g.,* nucleating agents, that alter the crystallization process can be used to influence the physical structure of the fiber, possibly improving its tensile performance.[7] Experimental work at Kimberly–Clark Corp., by Nohr and MacDonald,[8] demonstrated that the addition of fine-particle fumed silica to iPP does not result in an improvement in the tensile properties of spunbonded fabrics. However, under special conditions, dramatic increases in strength were realized upon addition of ultra-fine particle silica having a surface chemically modified so as to promote interactions with iPP. This article describes a systematic investigation of this phenomenon for the purpose of developing an understanding of the mechanism of action. Two approaches were used: (1) The nucleating ability, in iPP, of the surface-modified silica was investigated under quiescent conditions. Particular emphasis was placed on particle size reduction, to submicron sizes, and improved dispersion, accomplished in part by the use of a silicone copolymer fluid as a dispersing and anti-flocculation medium. This combination of ultrafine particle size and predispersion was tested for its ability to yield spunbonded fabrics with improved tensile properties. (2) The second method, used in conjunction with the first, was to optimize the melt flow index (MFI) and molecular weight distribution (MWD) of the iPP by blending various resins.

The use of silica as a nucleating agent has basis, in part, on previous reports that for several polymers silica affects the crystallization kinetics under quiescent conditions.[9–13] For example, the addition of a fumed silica to isotactic poly(propylene oxide) and poly(ethylene oxide) increased the number of primary nuclei during isothermal crystallization.[12,13] An increased nucleation density was obtained by decreasing the silica particle size, but the number of silica particles far exceeded the number of nuclei[9]; i.e., only a small fraction of the particles were active nucleating centers. This behavior was attributed to agglomeration of individual silica particles, due to hydrogen bonding, which reduces the number of particles that can become effective nucleating sites. It was also reported by Turturro et al.[9–11] that chemical modification of the surface of the silica particles reduces their effectiveness as nucleating agents for poly(ethylene terephthalate) and isotactic polystyrene. These studies were limited to crystallization under quiescent conditions and did not include work with iPP.

Lu and Spruiell[7] demonstrated that for spun filaments of iPP increasing the rate of quiescent crystallization causes crystallization to occur closer to the spinneret during processing and, thus, at a higher temperature. This results in a filament of lower tenacity and higher elongation-to-break. These effects were found to be most significant under conditions of low levels of stress (i.e., low "take up" velocities). Similarly, slower quiescent crystallization produced a filament of lower elongation-to-break but higher tenacity.

The role of MWD and MFI of iPP resin on the structure and properties of melt spun fibers was investigated in detail by Misra and co-workers,[14] although their importance had been suggested previously.[15–17] Under similar spinning conditions, increasing the weight average molecular weight, i.e., decreasing the MFI, while maintaining the MWD approximately constant produced a filament of higher modulus, tensile strength, and elongation-to-break. Similarly, within a set of resins with a given MFI, increasing the MWD produced a filament of higher modulus and elongation-to-break but of lower tensile strength.

EXPERIMENTAL

Sample Preparation

The iPP fibers and spunbonded fabrics were prepared as described previously.[18] In this investigation, the resin characteristics were changed by blending resin having an MFI of 5 with another having an MFI of 34 (i.e., Exxon 1052 and 3445, respectively). The content of lower MFI resin was varied between 45 and 60 wt %, but the fiber denier was maintained constant, between 1.6 and 1.8.

The process of fiber spinning was performed by first establishing the processing conditions using the "control" resin (Exxon 3445, MFI = 34). Subsequently, fiber spinning of the modified polymer systems was begun, with no modifications to instrument settings. This ensured identical processing conditions between the control system and the experimental formulations.

A poly(dimethylsiloxane) surface-modified silica, obtained from Cabot Corporation (Cab-O-Sil TS-720), was used in this investigation. The alkyl substitution on the poly(dimethylsiloxane) backbone was random, ranging from 2 to 11 methylene units. The size of the surface-modified silica parti-

Table I A Description of the Samples Used in This Investigation

	Description	
Sample	Polymer	Surface-Modified Silica/Silicone Copolymer Additive
PP34	Exxon 3445	none
PP5	Exxon 1052	none
C60/40	60% : 40% Blend of PP5/PP34	none
A0/100	Exxon 3445	0.3% (5% Silica in Silicone)
A45/55	45% : 55% Blend of PP5/PP34	0.3% (5% Silica in Silicone)
A50/50	50% : 50% Blend of PP5/PP34	0.3% (5% Silica in Silicone)
A55/45	55% : 45% Blend of PP5/PP34	0.3% (5% Silica in Silicone)
A60/40	60% : 40% Blend of PP5/PP34	0.3% (5% Silica in Silicone)

cles was reduced by ball milling (using 0.3 mm Draison rare earth grinding beads) for 3 h/100 g of silica at room temperature. The resulting surface-modified silica was dispersed in an alkyl silicone copolymer (Tegopren 6814, Goldschmidt, Richmond, VA) by mixing in a Draiswerke Motor Mill (Draiswerke Inc., Mahwah, NJ) for 15 min/L of silicone copolymer at temperatures ranging from room temperature to 80°C. The concentration of the surface-modified silica in the silicone copolymer fluid was maintained constant at 5%.

The surface-modified silica/silicone copolymer additive was dispersed in iPP using a twin screw extruder with several melt zones ranging in temperature from 190 to 200°C. Extrusion was performed at 70 rpm and a feed rate of 140 kg/h. The extruded iPP was cooled and cut into pellets which were subsequently used to produce the spunbonded fabrics. The content of the surface-modified silica/silicone copolymer in the final material was maintained constant at 0.3%, determined by separate experiments to be an optimal composition. These samples will be referred to as described in Table I.

Sample Characterization

Tensile Properties

Single fibers were mounted individually on cardboard test pieces previously cut to have a "C" shape. The fibers were mounted onto the cardboard form by gluing the ends. After the cardboard mount was clamped onto the Instron tensile tester (having a 1 g load cell) using pneumatic clamps it was cut, thereby leaving only the single fiber to be tested. The tensile deformation was performed at room temperature using an 8-cm fiber length and a 25 cm/min rate of pull. The reported values of the initial modulus, tensile strength, and elongation-to-break are the averages of 25 measurements. The grab tensile properties of the spunbonded fabrics were also determined at room temperature with an Instron tensile tester using a pull rate of 25 cm/min was on samples cut into a 10 $\times$ 15 cm test pieces, with the length cut in either the machine or in the cross direction. The reported values of the peak load, peak energy, and elongation-to-break are the averages of 10 measurements.

Spherulitic Growth Rates

A Nikon Optiphot optical polarizing microscope fitted with a Linkam THMS 600 hot stage and a Cohu video camera was used to observe isothermal crystallization rates. The apparatus and procedures have been described in detail previously.[19]

Differential Scanning Calorimetry

A Perkin–Elmer DSC-7C was used to determine the crystallization behavior of thin slices cut from iPP pellets (total weight of 3 to 4 mg). The samples were melted at 220°C for 15 min and quenched to the desired isothermal crystallization temperature, at a nominal rate of 300°C/min.

Electron Microscopy

The size distribution of the surface-modified silica particles as well as their dispersion in the silicone copolymer fluid and in iPP were investigated by bright field scanning transmittance electron mi-

croscopy (STEM) using a Jeol 100cx STEM microscope. The ultrafine particle silica was dispersed in methanol at a concentration of ~ 0.1%. A drop of the silica slurry was placed onto the surface of carbon-coated TEM hexagonal grids. The methanol was allowed to evaporate and the surface-modified silica particles were observed in bright field.

To investigate the dispersion of the surface-modified silica particles in the alkyl silicone copolymer, sections of the mixture were prepared by cryo-microtoming on a FC4 Reichert–Jung cryo-ultramicrotoming set at liquid nitrogen temperature. Thin slices of ~ 500 Å in thickness were collected and placed under vacuum (10^{-7} torr) at liquid nitrogen temperature. Gold was evaporated onto the surface at an angle of 30°. The sample was then transferred to the STEM and observed in bright field. Similarly, thin sections (400 Å) of the fibers were prepared by cryo-microtoming and the dispersion was investigated by observing the surface-modified silica particles in bright field. The method used to microtome the iPP fibers was the same as that described previously for the study of quench-cooled films.[20]

The STEM dark field investigation of the crystalline morphology of the iPP fibers and spunbonded fabrics was performed as described previously for the quench-cooled films.[20]

RESULTS AND DISCUSSION

Dispersion of the Surface-Modified Silica in iPP

The high magnification transmission electron micrograph of the surface-modified silica particles obtained after the ball milling procedure, presented in Figure 1, shows that it is composed of small primary particles. Some of these particles appear fused to each other, forming larger aggregates that range in size from < 0.1 μm to as large as 1 μm. The irregular shape of the particles precludes an accurate determination of the size distribution, but it is clear from the electron micrograph that the surface-modified silica powder is composed of submicron particles with a distribution in size.

The high magnification electron micrograph of the surface-modified silica particles dispersed in the alkyl silicone copolymer, presented in Figure 2, indicates a very good dispersion although the particle sizes remain unchanged from that observed in Figure 1. A distribution in the size is noted, with some indication of primary particles dispersed throughout the silicone copolymer. In addition, the bundles of particles that are observed in certain regions are consistent in size with the aggregates that were observed after it had been ball milled (Fig. 1). The surface-modified silica particles in the spun iPP fibers, seen as the black regions in Figure 3, are well dispersed within the iPP matrix and the size remains in the submicron range. Therefore, an important goal was realized in that the dispersion of the silica in the silicone copolymer prior to its incorporation into the iPP aided in maintaining the size of the ultrafine particle surface-modified silica.

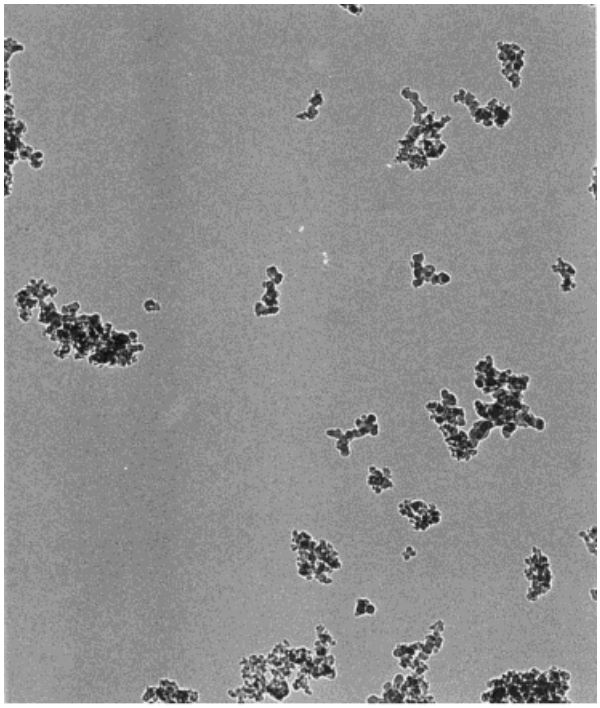

Figure 1 Electron micrograph of the surface-modified silica particles after ball milling for 3 h at room temperature (100,000×).

Crystallization Kinetics

In general, the progress of isothermal crystallization can be expressed by the Avrami treatment.[21–23] As simplified by Evans[24] and put into polymer context by Meares[25] and Hay[26] it has the form

$$\ln(1 - \chi_t) = -kt^n \qquad (1)$$

or

$$\log[-\ln(1 - \chi_t)] = \log k + n \log t \qquad (2)$$

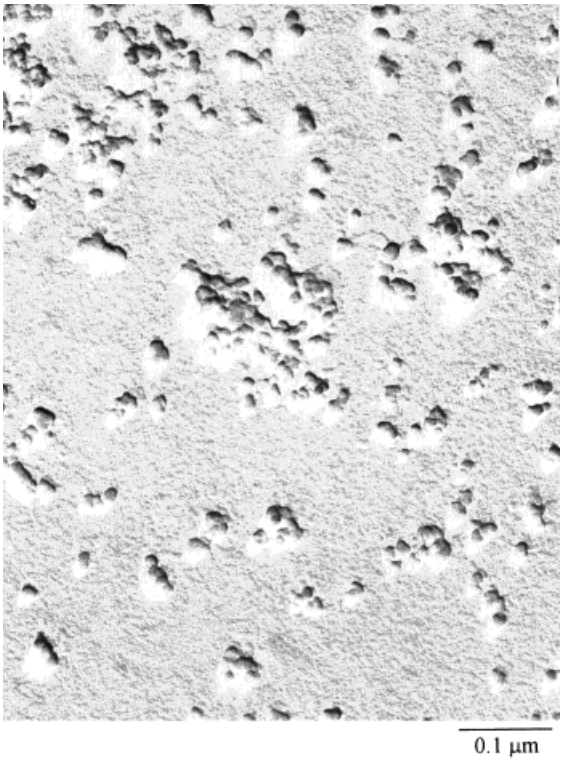

Figure 2 Electron micrograph of the surface-modified silica particles dispersed in the alkyl silicone copolymer (300,000×). The silica particles were dispersed in a Draiswerke motor mill for 1 h between room temperature and 80°C.

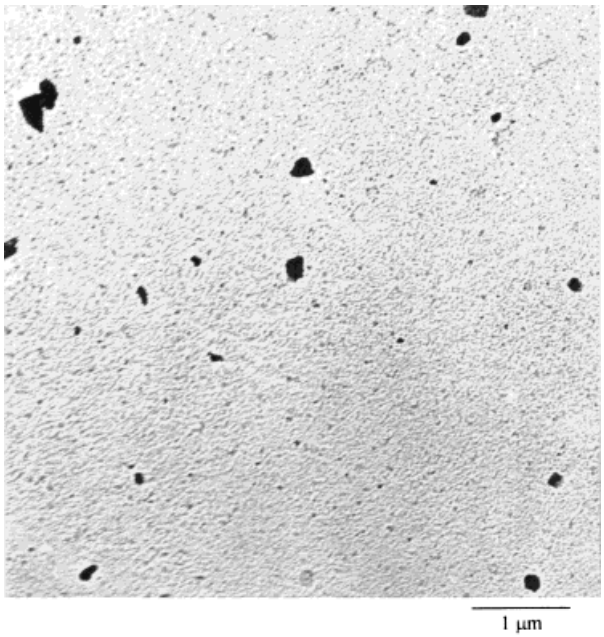

Figure 3 Bright field electron micrograph of the surface-modified silica particles dispersed in iPP (20,000×).

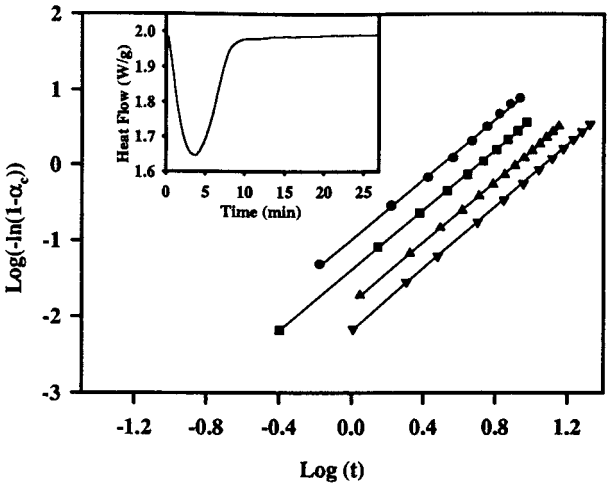

Figure 4 Avrami plot for isothermally crystallized PP34 at (circle) 120, (square) 122, (triangle) 124, and (inverted triangle) 126°C. (The inset is a typical DSC thermogram obtained upon isothermally crystallizing iPP).

where χ_t is the volume fraction of crystalline material or degree of crystallinity, k is the overall rate constant, n is an integer that depends on the mechanism of nucleation and on the form of crystal growth, and t is time. Due to different representations of the volume fraction of the crystalline phase, the form of k depends on the type of nucleation as well as on the form of the crystal growth.[26] In general, this rate constant is a combination of a nucleation density term and the growth rate of the crystalline entities.

The crystallization kinetics of iPP with and without the surface-modified silica/silicone copolymer additive were investigated by DSC under isothermal conditions in the range 120 to 126°C. A typical thermogram for the crystallization of PP34 is shown in the inset in Figure 4. The Avrami parameters, k and n, were derived from the $\log[-\ln(1 - \chi_t)]$ against $\log t$, as demonstrated in Figure 4. At all of the investigated crystallization temperatures, the Avrami index n was found to be nonintegral and to vary between 2 and 3 for both PP34 and PP5, as well as samples containing the surface-modified silica/silicone copolymer additive. These indices are in the lower portion of the range between 2.0 and 4.1 previously reported for iPP.[9,27] As discussed by Meares,[25] a nonintegral value for the Avrami index suggests that more than a single nucleation process or form of crystal growth is occurring simultaneously. Since iPP is a polymorphic material and heterogeneous and homogeneous nucle-

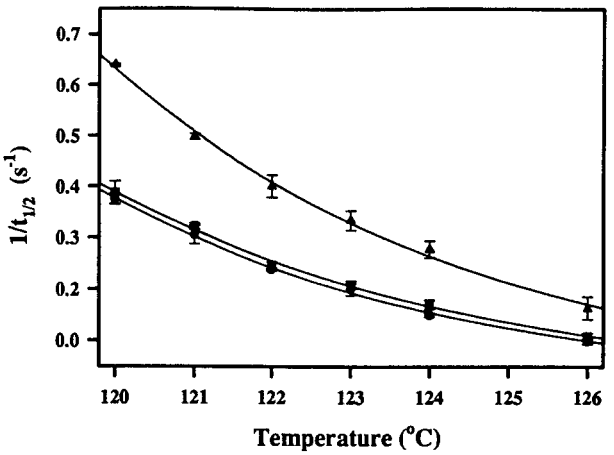

Figure 5 The inverse of the half-time of crystallization as a function of temperature for (circle) PP34, (square) PP5, and (triangle) a 60% : 40% blend of PP5/PP34 with the surface-modified silica/silicone copolymer additive.

ation can occur simultaneously, the value of n is unreliable in evaluating the nucleation and/or growth mechanism.

The overall rate of crystallization can be evaluated by noting the time for half of the crystallization, i.e., the point of 50% conversion, by the following relation:

$$t_{1/2} = [\ln 2/k]^{1/n} \qquad (3)$$

The overall rates, $(t_{1/2})^{-1}$, for resins PP34, PP5, and A60/40 are presented in Figure 5 for temperatures between 120 and 126°C. Although essentially the same rates of crystallization were obtained for PP34 and PP5, the addition of 0.3% of the surface-modified silica/silicone copolymer additive to the 60 : 40 blend of these two resins (i.e., A60/40) resulted in a dramatic increase in rate at all crystallization temperatures. This is quantitatively expressed by the overall rate constant, k, obtained from the double logarithmic plot (Fig. 6) which is substantially larger for the crystallization of the polymer system containing the surface-modified silica/silicone copolymer additive. Since this rate constant contains information concerning both nucleation and growth, the increased rate could be due to either of these parameters.

Radial growth rate measurements of individual spherulites were performed by optical microscopy at temperatures between 120 and 136°C for PP5 with and without the surface-modified silica/silicone copolymer additive. The data presented in Figure 6 clearly show that the spherulitic growth rates are unaffected by the presence of the additive. Hence, the observed increase in k, as well as in $(t_{1/2})^{-1}$, must result from an increase in the primary nucleation density providing unequivocal evidence that under isothermal conditions the surface-modified silica/silicone copolymer additive acts as a nucleating agent for iPP.

Isotactic Polypropylene Fibers

Tensile Properties

In this investigation, the evidence for enhancement in the tensile properties of iPP single fibers is based on a comparison with the tensile properties of fibers prepared from PP34. However, the resin characteristics were changed in some samples by blending this resin with a low MFI resin (i.e., PP5). The blending results in intermediate values of MFI, MWD, and average molecular weights (Table II). Since the tensile properties of

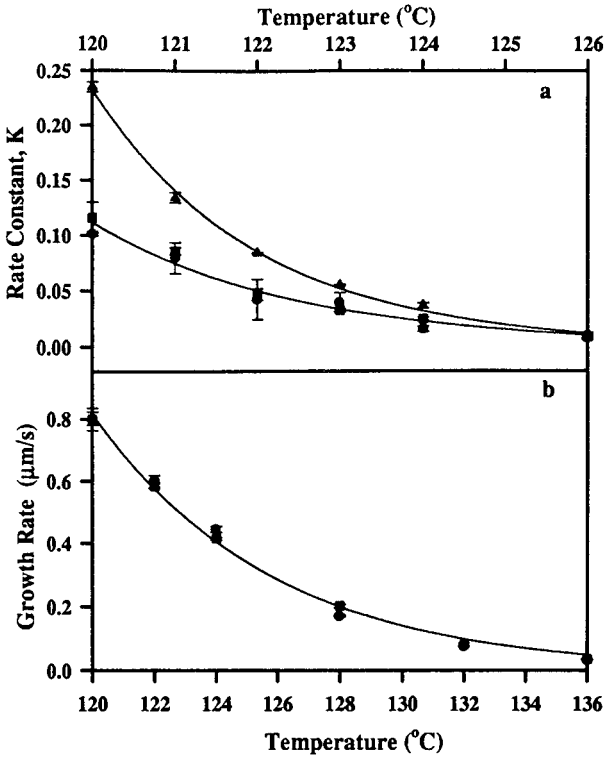

Figure 6 (a) Rate constant, k, obtained from the Avrami analysis of the isothermal crystallization of (circle) PP34, (square) PP5, and (triangle) a 60% : 40% blend of PP5/PP34 with the silica/silicone additive. (b) Temperature variation of the iPP spherulitic growth rate, (circle) PP5 and (square) PP5 with the surface-modified silica/silicone copolymer additive.

Table II MFI and Average Molecular Weights for PP34, PP5, and C60/40

Sample	MFI	$\bar{M}_n$	$\bar{M}_w$	$\bar{M}_z$	$\bar{M}_w/\bar{M}_n$
PP34	34	50,000	144,600	300,000	2.9
PP5	5	45,200	212,200	562,000	4.7
C60/40	18–20	46,200	158,800	404,600	3.4

the fibers are compared to those prepared from PP34, a comparison between the resin characteristics of PP34 and C60/40 indicates a decrease in the MFI and an increase in the resin MWD through a decrease in $\bar{M}_n$ and an increase in $\bar{M}_w$.

The tensile properties of iPP single fibers, 20 μm in diameter on the average, are presented in Table III. The initial modulus, tensile strength, and elongation-to-break are reported for three different iPP fibers; namely PP34, C60/40, and A60/40. The first two samples examine the effects of changing the resin characteristics. Indeed, decreasing the MFI and simultaneously increasing the MWD within the range reported in Table II does not affect the tensile properties of the resultant fibers.

Misra and co-workers[14] previously reported increases in the tensile properties of melt spun iPP fibers upon decreasing the MFI while maintaining the MWD approximately constant, and vice versa. However, those trends were noted as a result of large variations in the MFI and MWD, i.e., 19 to 95 in the former and 2.8 to 4.8 in the latter. These are substantially larger than the change in resin characteristics that was induced in this investigation through the blending of resins (Table II). However, of the nine iPP resins investigated by Misra and co-workers, two have characteristics (i.e., MFI and MWD) that are similar to those prepared in this study. For fibers prepared from those two resins, Mizra et al. report a small increase (60%) in the elongation-to-break while the modulus and tensile strength remained essentially unchanged.[14] A similar increase in elongation-to-break was not observed in this study, probably reflecting differences in processing conditions.

As seen from data in Table III, the presence of the surface-modified silica/silicone copolymer additive in the blend causes the initial modulus, tensile strength, and elongation-to-break to increase by 123, 77, and 221%, respectively, compared to those of fibers prepared from PP34. This improvement in tensile properties must be related to the nucleating effects of the additive that were observed under quiescent conditions.

Representative stress–strain curves for single fibers prepared from PP34 and A60/40, presented in Figure 7, clearly demonstrate significant differences in the tensile deformation properties. While the curve obtained for the fibers formed from PP34 resin indicates brittle fracture that for A60/40 fibers shows a "yield point" at $\sim$ 120% elongation, with no indication of "necking," followed by a plateau region which corresponds to permanent deformation at constant volume, or cold drawing. An increase in stress after this cold draw region is observed due to strain-induced crystallization, i.e., the alignment of elongated chains.[28] This pattern is similar to that of good elastomers. Therefore, the dispersion of the surface-modified silica/silicone copolymer additive system as well as possible concomitant effects from the addition of a low MFI resin modifies the tensile properties of the resultant fibers from behavior characteristics of brittle fracture to that of a good elastomer. This change in mechanical behavior must be related to changes in the morphology of the fibers that result from the addition of the nucleating agent for iPP.

Table III Tensile Properties of iPP Single Fibers

Sample	Diameter (μm)	Modulus (GPa)	Tensile Strength (MPa)	Elongation (%)
PP34	20.3 ± 0.6	2.1 ± 0.2	192 ± 38	198 ± 34
C60/40	19.2 ± 0.1	2.0 ± 0.2	162 ± 18	184 ± 22
A60/40	21 ± 1	4.7 ± 0.3	340 ± 23	636 ± 26

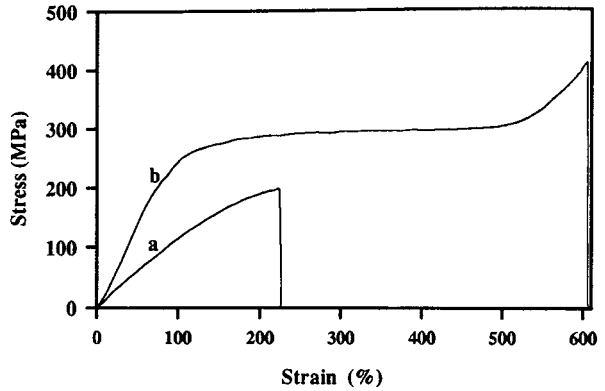

Figure 7 Stress–strain curves for iPP single fibers prepared from (a) PP34 and (b) A60/40.

Morphology of iPP Fibers

The crystalline phase of the melt spun fibers was investigated by STEM in cryo-microtomed sections that were sliced in both the longitudinal and cross-sectional directions. The STEM dark field images for resin A60/40 (Fig. 8) indicate that in the longitudinal direction the crystalline phase is oriented in the fiber direction, as is clearly seen by the elongated white regions. In the cross-sectional direction, small crystalline regions are noted throughout the micrograph. The combination of the longitudinal and cross-sectional micrographs suggests that the crystalline morphology is consistent with a fibrillar or cylindritic type of supermolecular structure.[29]

The crystal sizes observed in the cross-sectional direction were measured at the surface, mid-radius, and core of the fiber. The crystalline entities in the fibers prepared from PP34 were found to be essentially constant in size from the surface to the core of the fiber, ranging between 120 and 170 Å, with an average of 140 Å. By comparison, for fibers prepared from the A60/40 resin the crystal sizes varied from the surface to the core of the fiber: at the surface, the crystals were substantially smaller, ranging in size from 25 to 70 Å, with an average of 40 Å; the average crystal size increased to 70 Å at the mid-radius and finally to 160 Å in the core. It is of interest that the crystal sizes at the core are similar to those observed in the fibers prepared from only PP34. The surface-modified silica/silicone copolymer additive induces a definite skin to core variation in morphology that is not apparent in PP34, and the decrease in crystal size at the surface and mid-radius must be directly related to the nucleating effects of the silica/silicone additive. This effect cannot be due to differences in processing conditions since they were maintained constant during the process of fiber spinning.

In an investigation of spider dragline elasticity, Termonia[30] introduced a comprehensive molecular model that incorporates most of the information known to date about the structure of such fibers. This model is based on previous analyses of the factors that control the deformation of polyethylene fibers.[31–34] The fibers are viewed as a semicrystalline material composed of amorphous flexible chains reinforced by strong, stiff crystals. A third region is described which has properties similar to the interfacial region in semicrystalline polymers. It was suggested that a thin layer surrounding the β-sheets is formed in the amorphous phase that has a modulus of elasticity higher than that of the bulk. Although motion is hindered, the chains in this region do not lose their extensibility.

Among other matters, Termonia investigated

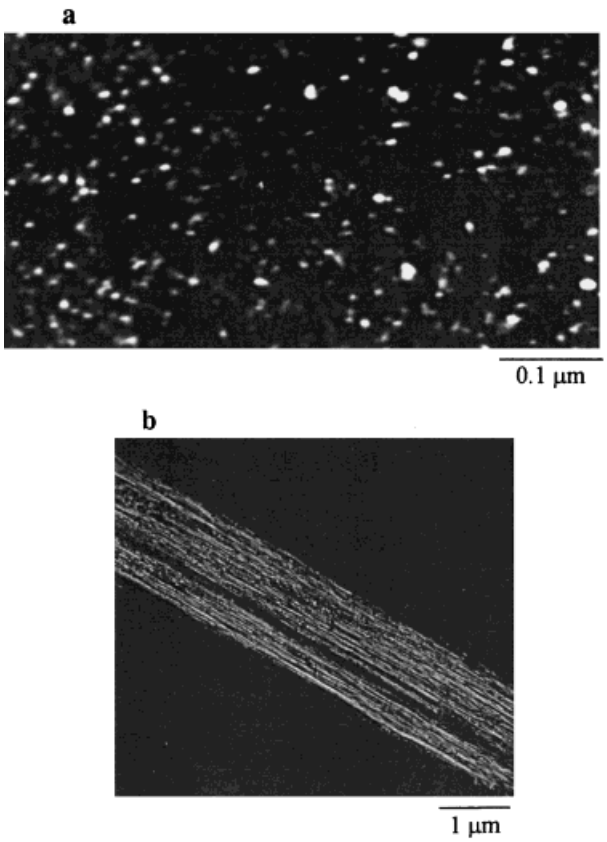

Figure 8 STEM dark field image of n-beam reflections of an iPP fiber prepared from a 60% : 40% blend of PP5/PP34 with the silica/silicone additive: (a) cross-sectional cut (300,000×), (b) longitudinal fiber section cut close to the fiber surface (10,000×).

the role of the crystallite size on the tensile strength of the fibers and on the formation of the thin, high modulus layer that surrounds the crystallites.[30] It was demonstrated that decreasing the size of the crystallites while maintaining a constant crystalline volume fraction leads to a substantial increase in tensile strength of the fibers. This increase in tensile strength was found to be due to the concomitant increase in the volume fraction of the thin, high modulus layer surrounding the crystals, i.e., the interfacial region, which effectively reinforces the fiber and increases its tensile strength. This effect is similar to that of the thin interface of constrained mobility that is generated in the carbon black reinforcement of rubbers.[35]

The improved tensile properties obtained in the present investigation appear to result from a similar reduction in the size of the crystalline entities. The surface-modified silica/silicone copolymer additive nucleates the iPP and effectively reduces the size of the crystals at the skin and mid-radius of the fibers. This decrease in crystal size increases the volume fraction of the interfacial phase and enhances the tensile strength of the fibers. However, the effect of the resin molecular weight must also be considered. The concomitant effect of a reduced crystal size and increased molecular weight is expected to promote the generation of a greater number and a more even distribution of "tie" molecules in the fiber. This will also enhance its tensile strength. Therefore, the lower MFI and broader MWD distribution, for the fibers that also contain the surface-modified silica/silicone copolymer additive, probably also contribute synergistically to the enhancement of the tensile strength.

Spunbonded Fabrics

Tensile Properties

It is well known that the properties of the spunbonded fabrics are greatly dependent on the processing and thermal bonding conditions. In the course of this investigation, several lots of fibers and spunbonded fabrics were prepared with resin PP34. In all cases, the tensile properties of these fibers were found to be in the range that is listed in Table III. However, the tensile properties of the derived spunbonded fabrics were found to differ significantly from one sample to the next, undoubtedly due to differences in the thermal bonding conditions which affect the quality of the bond points. This is clearly evident from a comparison of the tensile properties of the two PP34 spunbonded fabrics listed in Table IV. Consequently, a comparison of the fabric tensile properties must be performed with fabrics that were processed and thermally bonded under the same conditions. Therefore, the two sets of data that are separated in Table IV should not be compared directly.

The dispersion of the surface-modified silica/silicone copolymer additive system in the iPP blend systems results in a dramatic increase in the tensile properties of the spunbonded fabrics in both the machine and cross direction compared to the fabrics prepared from PP34 (Table IV). In addition, a gradual improvement in all properties is noted as the concentration of the lower MFI resin, PP5, is increased from 45% to 60%. It should be noted that, due to viscosity constraints, it was not possible to spin fibers from resin blends with higher concentrations of the lower MFI resin. Increases as high as 82, 210, and 81% in the peak load, peak energy, and elongation-to-break, respectively, were noted for the A60/40 spunbonded fabrics. In the iPP blend systems the surface-modified silica/silicone copolymer additive results in spunbonded fabrics of substantially increased tenacity.

The second set of data in Table IV indicate that the dispersion of the surface-modified silica/silicone copolymer additive in PP34 (i.e., A0/100) results in only moderate increases in the tensile properties of the resultant spunbonded fabric compared to those fabrics prepared from PP34. Increases of 30 to 40% are noted in the peak load and peak energy while the elongation-to-break remains essentially constant. Similarly, a comparison of the tensile properties of spunbonded fabrics that were prepared from C60/40 and PP34 indicates a moderate increase in peak load while the peak energy and elongation-to-break remain essentially unchanged.

In the spunbonded fabrics prepared with PP34, the surface-modified silica/silicone copolymer additive induces moderate increases in tensile performance. The increases in peak load and energy for these samples are substantially smaller than those observed for the blend systems containing surface-modified silica/silicone copolymer additive. Similarly, spunbonded fabrics prepared from C60/40 show only small increases in peak load. This is consistent with the observations that were made for the C60/40 and PP34 single fibers. However, when the surface-modified silica/silicone copolymer additive is dispersed in the blend of iPP resins, a

Table IV Tensile Properties of the Spunbonded iPP Fabrics

	Peak Load (kg)		Peak Energy (kg^{-1} m^{-1})		% Elongation	
Sample	M.D.	C.D.	M.D.	C.D.	M.D.	C.D.
PP34	14 ± 1	11 ± 0.7	0.36 ± 0.06	0.29 ± 0.05	58 ± 4	62 ± 6
A45/55	18 ± 0.9	16 ± 0.6	0.85 ± 0.08	0.72 ± 0.09	96 ± 7	98 ± 7
A50/50	19 ± 1.5	16 ± 0.8	0.88 ± 0.1	0.71 ± 0.09	97 ± 4	101 ± 8
A55/45	20 ± 1.4	18 ± 0.9	0.90 ± 0.09	0.79 ± 0.08	99 ± 8	102 ± 8
A60/40	21 ± 1.5	20 ± 0.8	0.99 ± 0.09	0.90 ± 0.07	105 ± 8	108 ± 9
PP34	10 ± 0.6	8 ± 0.3	0.26 ± 0.03	0.29 ± 0.02	44 ± 4	44 ± 4
A0/100	13 ± 0.5	11 ± 0.4	0.34 ± 0.02	0.28 ± 0.04	45 ± 3	46 ± 4
C60/40	15 ± 0.8	12 ± 1	0.30 ± 0.02	0.29 ± 0.01	45 ± 3	47 ± 4

M.D., machine direction; C.D., cross direction.

more pronounced increase in tensile properties is observed. Furthermore, these tensile properties are dependent on the concentration of the low MFI resin. It appears that the improvement in the tensile properties is a consequence of the nucleating ability of the surface-modified silica/silicone copolymer additive as well as the decrease in MFI and broadening of the MWD. While neither of these

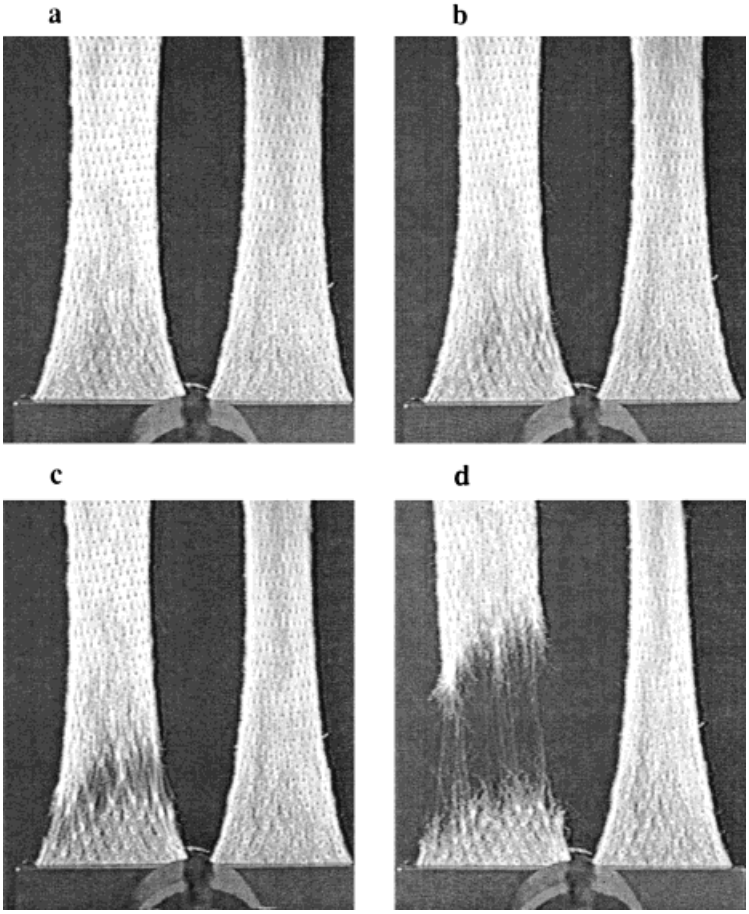

Figure 9 Photographs of the spunbonded fabrics at different times during tensile deformation: left-hand side sample, PP34; right-hand side sample, A60/40.

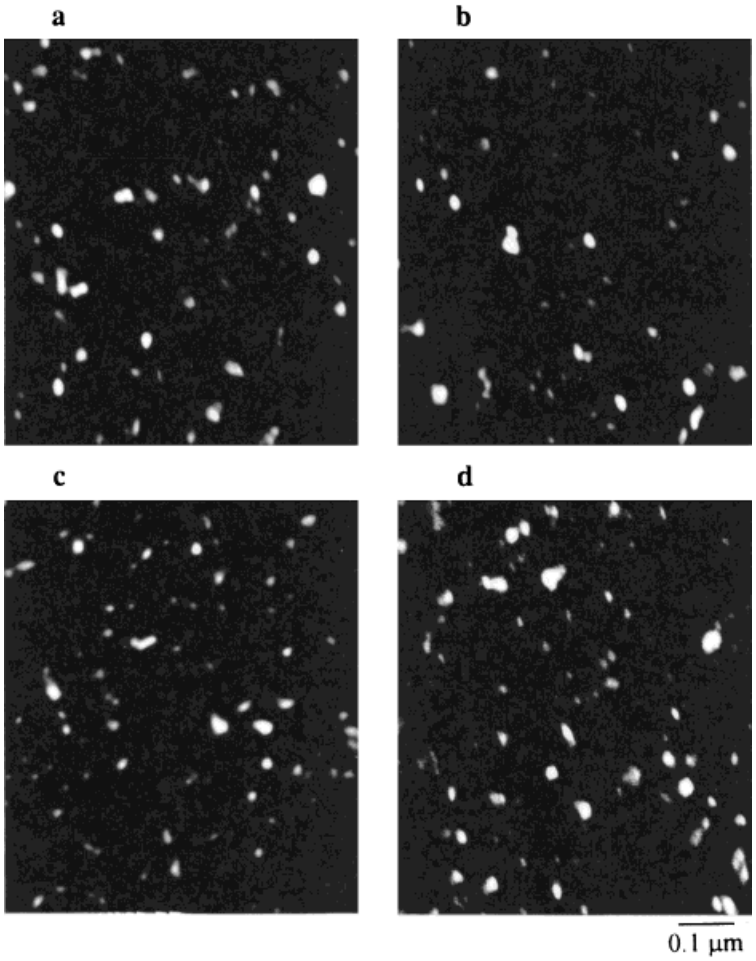

Figure 10 STEM dark field image of n-beam reflections of a cross-sectional cut of the bond point of a spunbonded fabric prepared from PP34 (100,000×): (a) edge of the bond point, (b) 200, (c) 400, and (d) 600 Å from the edge of the bond point.

changes independently results in substantial improvements of the tensile properties of the spunbonded fabrics, in combination they act synergistically to produce dramatic increases.

A video recording was made to study the tensile deformation of the spunbonded fabrics. Photographs selected from the video images, presented in Figure 9, show the results at various times during the tensile deformation. The spunbonded fabric seen on the left-hand side of each photograph is fabric formed from resin PP34, while the one on the right-hand side is from A60/40. These photographs clearly demonstrate the enhancement in elongation-to-break that was achieved in the A60/40 fabrics. Even after failure has occurred in the PP34 spunbonded fabric (Fig. 9C), extension continues in the A60/40 fabric.

Close inspection of the failure zone of the PP34 spunbonded fabric (Fig. 9C) reveals that the bond points, seen as the small squares, remain intact during failure in the fabric, suggesting that the failure results from failure either in the fibers or at the bond point–fiber interface. However, the PP34 fabric fails at an elongation-to-break of $\sim 60\%$ (Table IV), i.e., at elongations substantially smaller than the 200% obtained for the single fibers (Table III). This would tend to indicate that failure is occurring at the bond point–fiber interface. This has been suggested previously[3–6] and appears to be generally accepted in the industry. The heat and pressure treatment that is used during thermal bonding may generate morphology changes (e.g., size of crystallites) at the interface that cause it to become most susceptible to failure.

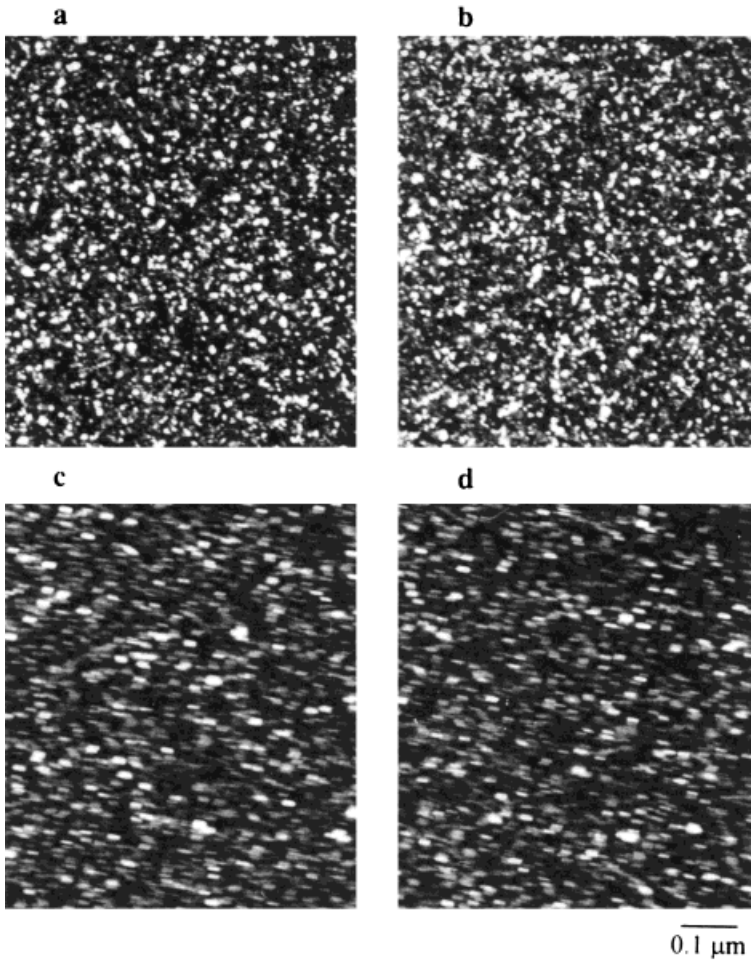

Figure 11 STEM dark field image of n-beam reflections of a cross-sectional cut of the bond point of a spunbonded fabric prepared from A60/40 (100,000×): (a) edge of the bond point, (b) 200, (c) 400, and (d) 600 Å from the edge of the bond point.

Morphology of Spunbonded Fabrics

The bond points in the spunbonded iPP fabrics PP34 and A60/40 were investigated by STEM using cryo-microtomed sections sliced in the cross-sectional direction. The corresponding dark field images that illustrate the crystalline phase at various locations within the bond point are shown in Figures 10 and 11, respectively. Micrographs of cross-sectional cuts are presented for positions located at 200 Å intervals, beginning at the bond point edge.

As for the iPP fibers, the presence of the silica/silicone additive in the resin blend results in a reduction in size of the crystallites within the bond points and a concomitant increase in the nucleation density so that the overall degree of crystallinity is essentially unchanged. In both of these samples the size and density of the crystallites appear to remain essentially constant across the bond point. The reduction in crystal size and increase in nucleation density are in accord with the nucleating ability of the surface-modified silica/silicone copolymer additive.

The formation of the bond points was performed by a hot calendering technique which involves heating and laterally compressing the fibers. The substantially smaller crystal sizes at the surface of the A60/40 fibers should favor the bonding process. Due to the smaller crystallite sizes on the surface of these fibers, a greater fraction of these crystallites will fuse at a given bonding temperature. Upon cooling, this melted fraction crystallizes with increased nucleation density due to the presence of the surface-modified silica/silicone copolymer additive. The combination of these two effects should result in improved bonding of the iPP fibers. Furthermore, separate studies showed a smoother transition in the morphol-

ogy at the interface between the bond point and fibers of the additive-containing fabrics, further contributing to a reduced likelihood of failure at this interface. The net result is the improved elongation-to-break properties of the fabric.

SUMMARY AND CONCLUSIONS

The effectiveness of surface-modified silica as a nucleating agent for iPP is markedly improved by a decrease in size. By use of a silicone copolymer dispersing medium such ultrafine particle silica can be dispersed uniformly in iPP, with minimal agglomeration, even with low shear mixing in an extruder. Under isothermal conditions, the surface-modified silica/silicone copolymer additive increases the overall rate of crystallization by acting as an efficient nucleating agent. The number of primary nuclei increases while the radial growth rate of individual spherulites is unaffected.

The addition of the surface-modified silica/silicone copolymer mixture to the blend of iPP resins, at a level of only 0.1 wt %, resulted in improved tensile properties in both the iPP fibers and spunbonded fabrics. At the highest concentration of the low MFI resin in the blend, i.e., 60%, increases of 82, 210, and 81% in peak load, peak energy, and elongation-to-break, respectively, were achieved in the spunbonded fabrics compared to fabrics prepared from PP34. Similarly, in the iPP fibers, an increase of 123, 77, and 221% was achieved in the initial modulus, tensile strength, and elongation-to-break, respectively, relative to fibers prepared from PP34. In addition, while the tensile deformation of the fibers prepared from PP34 indicates brittle fracture, the fibers prepared from A60/40 are consistent with the stress–strain behavior of a good elastomer.

The improved tensile properties of both the iPP fibers and spunbonded fabrics were found to be due to a combination of the nucleating ability of the silica/silicone additive, reflected by a substantially smaller crystallite size, and the lower MFI and broader MWD that were achieved in the iPP resin from the blending of two resins with different MFI. The smaller crystal sizes in the fibers and bond points induce more homogeneously distributed crystallites within the amorphous phase, without a significant change in overall crystallinity. The combination of the smaller crystal sizes and the higher molecular weight is favorable to the development of a greater number and better distribution of load-bearing "tie" molecules, which results in an increase in tensile strength, modulus, and elongation-to-break.

Financial support in the form of operating grants (GRB) and scholarships (VC) from the Natural Sciences and Engineering Research Council of Canada (NSERC) and les Fonds pour la Formation et l'Aide à la Recherche (Fonds FCAR) of Québec is gratefully acknowledged.

REFERENCES

1. S. B. Warner, *Text. Res. J.,* **59,** 151 (1989).
2. P. E. Gibson and R. L. McGill, *Tappi.* 82 (1987).
3. F. Harris, *IMPACT 85,* V1-V38, Ft. Lauderdale, 1985.
4. S. B. Warner, *ANTEC,* paper 33-137, Atlanta, 1988.
5. J. G. Tomka, in *Comprehensive Polymer Science, The Synthesis, Characterization, Reactions & Applications of Polymers,* G. Allen, Ed., Pergamon Press, Oxford, 1989, p. 487.
6. J. Zimmerman, in *Comprehensive Polymer Science, The Synthesis, Characterization, Reactions & Applications of Polymers,* G. Allen, Ed., Pergamon Press, Oxford, 1989, p. 249.
7. F. M. Lu and J. E. Spruiell, *J. Appl. Polym. Sci.,* **49,** 623 (1993).
8. R. S. Nohr and J. G. MacDonald, Kimberly–Clark Corp., unpublished results, 1990.
9. G. Turturro, Ph.D. Thesis, McGill University, Montreal, Quebec, 1981.
10. G. Turturro, G. R. Brown, and L. E. St-Pierre, *Polymer,* **25,** 659 (1984).
11. G. Turturro and L. E. St-Pierre, *J. Colloid Interface Sci.,* **67,** 349 (1978).
12. J. H. Cole, Ph.D. Thesis, McGill University, Montreal, Quebec, 1977.
13. J. H. Cole and L. E. St-Pierre, *ACS Symposium Series,* **6,** 58 (1975).
14. S. Misra, F.M. Lu, J. E. Spruiell, and G. C. Richeson, *J. Appl. Polym. Sci.,* **56,** 1761 (1995).
15. F. Lu and J. E. Spruiell, *J. Appl. Polym. Sci.,* **34,** 1521 (1987).
16. F. Lu and J. E. Spruiell, *J. Appl. Polym. Sci.,* **34,** 1541 (1987).
17. Q. Fan, D. Xu, D. Zhao, and R. Qian, *J. Polym. Eng.,* **5,** 95 (1985).
18. V. Caldas, G. R. Brown, J. G. MacDonald, and R. S. Nohr, *J. Polym. Sci., Polym. Phys. Ed.,* **34,** 2085 (1995).
19. K. L. Singfield and G. R. Brown, *Macromolecules,* **28,** 1290 (1995).

20. V. Caldas, G. R. Brown, R. S. Nohr, J. G. MacDonald, and L. E. Raboin, *Polymer,* **35,** 899 (1994).
21. M. Avrami, *J. Chem. Phys.,* **7,** 1133 (1939).
22. M. Avrami, *J. Chem. Phys.,* **8,** 212 (1940).
23. M. Avrami, *J. Chem. Phys.,* **9,** 177 (1941).
24. U. R. Evans, *Trans. Faraday Soc.,* **41,** 365 (1945).
25. P. Meares, *Polymers: Structure and Bulk Properties,* Van Nostrand, New York, 1965, Chap. 5.
26. J. N. Hay, *Br. Polym. J.,* **3,** 74 (1971).
27. P. Parrini and G. Corrieri, *Makromol. Chem.,* **62,** 83 (1963).
28. I. M. Ward, *Mechanical Properties of Solid Polymers,* Wiley, New York, 1971, Chap. 11.
29. J. Varga, in *Polypropylene Structure, Blends and Composites,* Vol. 1, J. Karger-Kocsis, Ed., Chapman and Hall, London, 1995, p. 91.
30. Y. Termonia, *Macromolecules,* **27,** 7378 (1994).
31. Y. Termonia and P. Smith, *Macromolecules,* **20,** 835 (1987).
32. Y. Termonia and P. Smith, *Macromolecules,* **21,** 2184 (1988).
33. Y. Termonia and P. Smith, *Macromolecules,* **21,** 3485 (1988).
34. Y. Termonia and P. Smith, *Macromolecules,* **26,** 3738 (1993).
35. J. B. Donnet and A. Vidal, *Pharmacy, Thermomechanics, Elastomers, Telechelics,* K. Dusek, Ed., Springer-Verlag, Berlin, 1986, p. 104.